Modulating the Bioactivity of Mucin Hydrogels with Crosslinking Architecture

Kun Jiang, Hongji Yan, Carolin Rickert, Matthias Marczynski, Kajsa Sixtensson, Francisco Vilaplana, Oliver Lieleg, and Thomas Crouzier*

Hydrogels made of crosslinked macromolecules used in regenerative medicine technologies can be designed to affect the fate of surrounding cells and tissues in defined ways. Their function typically depends on the type and number of bioactive moieties such as receptor ligands present in the hydrogel. However, the detail in how such moieties are presented to cells can also be instrumental. In this work, how the crosslinking architecture of a hydrogel can affect its bioactivity is explored. It is shown that bovine submaxillary mucins, a highly glycosylated and immune-modulating protein, exhibit strikingly different bioactivities whether they are crosslinked through their glycans or their protein domains. Both the susceptibility to enzymatic degradation and macrophage response are affected, while rheological properties and barrier to diffusion are mostly unaffected. The results suggest that crosslinking architecture affects the accessibility of the substrate to proteases and the pattern of sialic acid residues exposed to the macrophages. Thus, modulating the accessibility of binding sites through the choice of the crosslinking strategy appears as a useful parameter to tune the bioactivity of hydrogel-based systems.

1. Introduction

Mucins are a group of glycoproteins anchored to the cell membrane or secreted by epithelial cells to form the mucus gels covering the wet epithelium surfaces of the nose, mouth, stomach, lungs, intestinal tract, and female reproductive tract. Mucins play a central role in the barrier, hydration, and lubrication functions of mucus. Mucins are also bioactive,[1] regulating the activities of immune cells by binding to surface receptors[2,3] and interacting with bioactive proteins and peptides.[4–7] With our knowledge of mucin structure and functions improving over the last decades, mucin has increasingly been investigated as a building block of biomaterials that can recapitulate key functions of mucus.[1] Mucins purified from mucosal tissues of animals such as stomach and submaxillary glands have been assembled into coatings[8,9] and films[10,11] that exhibit the lubricative, antifouling, and drug binding properties of mucins. Gel-forming mucins can self-assemble into hydrogels under certain conditions driven by intermolecular cross-linking by noncovalent bonds.[12,13] However, this spontaneous gelation is difficult to control and typically leads to weak gels, thus limiting their applications. More robust hydrogels can be obtained by covalently crosslinking the mucins to each other or by blending with mucoadhesive molecules.[14–16]

In our recent work, we showed that cross-linked bovine submaxillary mucin (BSM) hydrogels could modulate the activity of macrophages cultured at their surfaces in vitro[17] and modulate the foreign body reaction after implantation in vivo, inhibiting their fibrotic encapsulation.[18] Such mucin hydrogels

K. Jiang, Dr. H. Yan, K. Sixtensson, Prof. F. Vilaplana, Dr. T. Crouzier
Division of Glycoscience
Department of Chemistry
School of Engineering Sciences in Chemistry
Biotechnology and Health
KTH
Royal Institute of Technology
AlbaNova University Center
Stockholm 106 91, Sweden
E-mail: crouzier@kth.se

The ORCID identification number(s) for the author(s) of this article can be found under https://doi.org/10.1002/adfm.202008428.

K. Jiang, Dr. H. Yan, Dr. T. Crouzier
AIMES – Center for the Advancement of Integrated Medical
and Engineering Sciences at Karolinska Institutet
and KTH Royal Institute of Technology
Stockholm 114 28, Sweden

K. Jiang, Dr. H. Yan, Dr. T. Crouzier
Department of Neuroscience
Karolinska Institutet
Stockholm SE-171 77, Sweden

C. Rickert, M. Marczynski, Prof. O. Lieleg
Department of Mechanical Engineering and Munich
School of Bioengineering
Technical University of Munich
Boltzmannstrasse 15, 85748 Garching, Germany

C. Rickert, M. Marczynski, Prof. O. Lieleg
Center for Protein Assemblies
Technical University of Munich
Ernst-Otto-Fischer Str. 8, 85748 Garching, Germany
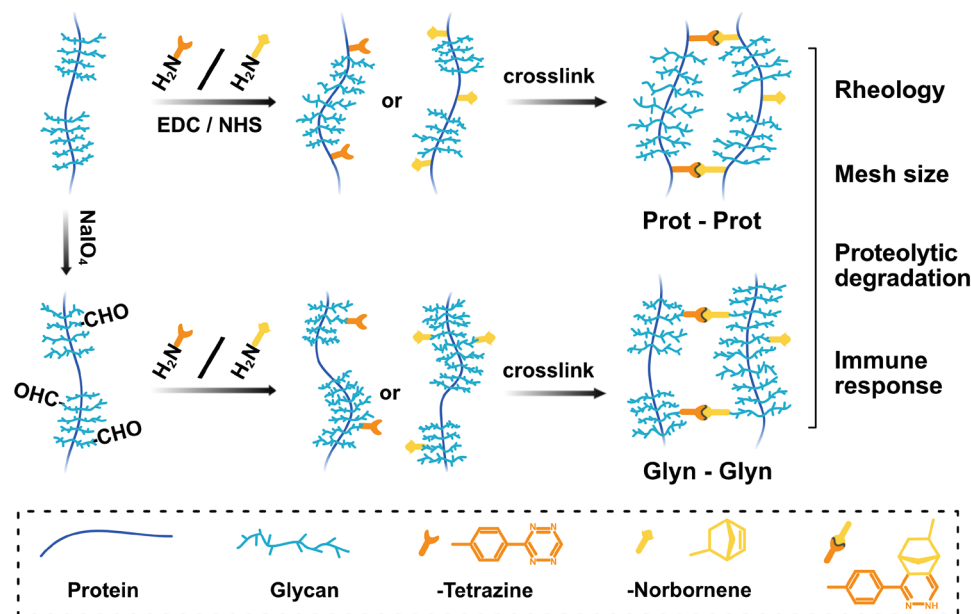
Figure 1. Illustration of mucin modification with tetrazine and norbornene on protein backbone or on glycan chains. The crosslinked mucin gels by protein backbone (Prot-Prot) and by glycan side chain (Glyn-Glyn) have a different performance with macrophage and enzyme treatments.

could improve therapies currently limited by excessive fibrosis, including cell transplantation, and sensor or electrode implantation. Our work[17] and the work of others[19,20] suggest that the immune-modulating capacity of these mucin hydrogels seem to be largely driven by the presence of sialic acid residues present as a capping sugar on the BSM glycosylation. Sialic acid and other sugars present in BSM can interact with cell surface receptors such as Siglecs[21,22] and scavenger receptors[23] and trigger intracellular signaling.[24]

While the bioactivity of these mucin gels are being further investigated, it is also of interest to explore ways in which such activity can be controlled and modulated. One approach to modulate such activity is to change the glyco-composition of the mucins, for instance by enzymatic addition or removal of sugars.[17] Another strategy to modulate the bioactivity of mucin gel is to alter the accessibility of the glycan ligands to receptors. For example the fibroblast growth factor (FGF)[25] and bone morphogenetic protein (BMP)[26,27] exhibit very different bioactivities whether they are presented in solutions or in the solid phase, for instance bound to materials. The importance of ligand presentation was also suggested for mucin coatings, which interacted differently with bacteria depending on the site by which the molecule was attached to the surface.[28,29] Thus, we hypothesize that the architecture of the hydrogel could affect its bioactivity by affecting ligand density, adding or removing steric hindrances to interactions, or allowing the co-presentations of new ligands. The architecture of a hydrogel can be tuned by the details of the chemical crosslinking of the components.[30] For example, the choice of crosslinking chemistry applied to collagen materials was shown to modulate their in vitro inflammatory responses[31] and crosslinking densities can affect integrin-mediated cell adhesion.[32]

In this work, we investigate whether varying the position of the crosslinks on mucins would affect material properties and

bioactivity of the resulting hydrogel. Mucins can be described as bottlebrush structures (**Figure 1**). Crosslinks can be placed either on the protein "core" or on the oligo-saccharides "brush." We use tetrazine (Tz) and norbornene (Nb) modified bovine submaxillary mucins that spontaneously form stable hydrogels when mixed.[18,33] We localize crosslinks on the mucin core (Protein-Protein crosslinking, or Prot-Prot) using EDC/NHS coupling and compare to brush-based crosslinking (Glycan-Glycan crosslinking, or Glyn-Glyn) achieved using periodate oxidation, which mediates the formation of reactive aldehyde on the sugars of the mucins (Figure 1). By comparing Prot-Prot to Glyn-Glyn crosslinking, we find that the crosslink localization had a mild effect on the rheological and barrier properties of the resulting gels, but strongly impacted their susceptibility to protease degradation and their bioactivities as suggested by the response of macrophages to the gel.

2. Results and Discussion

2.1. Mucins can be Crosslinked by their Glycans while Retaining Most of the Sialic Acid Residues Intact

To crosslink the mucins through their glycan side chains, we first generated reactive aldehyde groups by mild sodium periodate oxidation. Similar approaches have been successfully attempted before with dextran polysaccharide cross-linked to gelatin.[34] The aldehydes were then reacted with Nb and Tz derivatives to yield Glyn-BSM-Nb and Glyn-BSM-OTz, respectively. Periodate oxidation mainly breaks the bond between adjacent hydroxyls of mucin associated sugars and sialic acid is specifically sensitive to periodate oxidation under mild conditions (Figure S1, Supporting Information).[35] In addition to the predominant Neu5Ac form of sialic acid,[36] BSM also contains
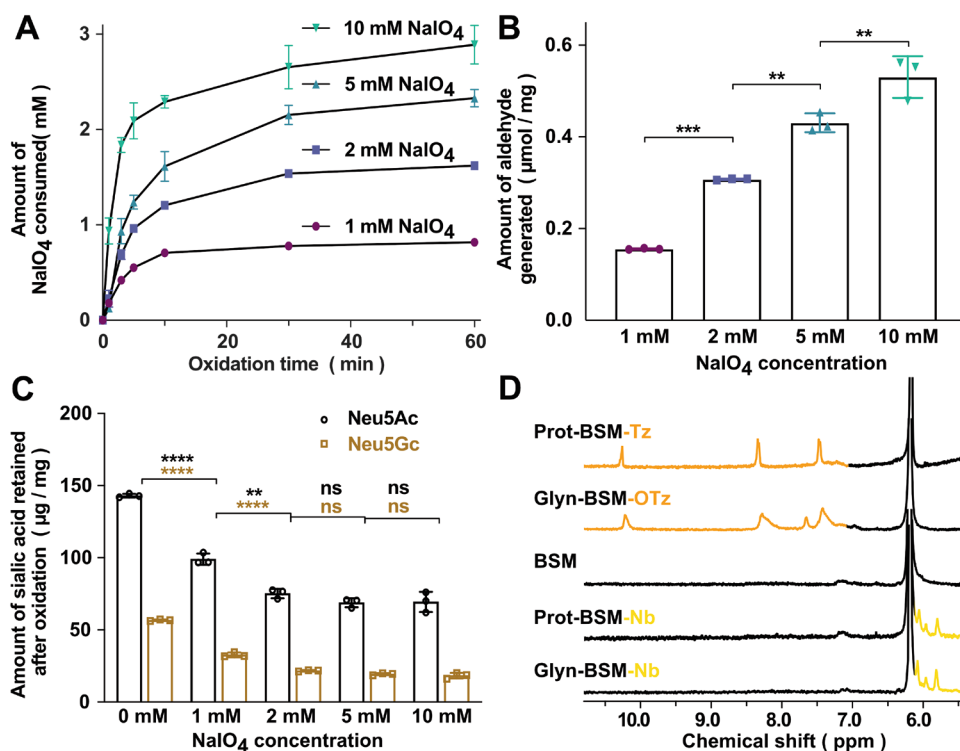
Figure 2. A) The amount of NaIO$_4$ consumed over 60 min with different concentration of NaIO$_4$, B) the quantity of aldehyde groups per mg BSM generated after oxidation based on the assumption that the consumption of one NaIO$_4$ leads to one aldehyde group, C) the remaining sialic acid contents of Neu5Ac and Neu5Gc per mg BSM after oxidation and the D) NMR spectrums of BSM and functionalized BSM. Statistical significance was calculated by one-way ANOVA test by Prism 8.0. *, **, ***, and **** indicate p values of <0.05, 0.01, 0.0005, and 0.0001, respectively.

a minority of glycolylated sialic acid Neu5Gc which is not found in human tissues.[37] Both sialic acid variants can confer materials with bioactivity by binding to Siglec cell surface receptors on immune cells,[38] albeit with different affinities.[39,40] Excessive oxidation could degrade a significant proportion of both sialic acids and affect the bioactivity of the material.[19,41]

We thus first optimized the mucin oxidation by varying reaction time and sodium periodate concentrations. We found that the oxidation ran to equilibrium within 60 min for all periodate concentrations. The amount of periodate consumed at 60 min (**Figure 2**A), and thus the amount of aldehyde generated (Figure 2B), increased with periodate concentration from 1 to 10 mм. The remaining sialic acid contents of mucin after oxidation, Neu5Ac and Neu5Gc, were tested by high-performance anion-exchange chromatography (HPAEC). The amount of Neu5Ac decreased by about 31% and 48% after oxidation with 1 and 2 mм sodium periodate for 30 min, respectively. The amount of Neu5Ac decreased further with higher sodium periodate concentrations at 5 and 10 mм (Figure 2C and Figure S2: Supporting Information). Neu5Gc was affected similarly, with a decrease by about 44% and 61% after oxidation with 1 and 2 mм sodium periodate, and no further decrease with 5 and 10 mм sodium periodate. Interestingly, Neu5Gc was more affected than Neu5Ac by the sodium periodate oxidation, with a 44% decrease in Neu5Gc compared to 30% decrease for Neu5Ac at 1 mм sodium periodate and a 61% decrease in Neu5Gc compared 48% decrease in Neu5Ac at 2 mм sodium periodate. This result is consistent with a previous

report that suggested higher susceptibility of Neu5Gc to sodium periodate oxidation[42] and of fraction of Neu5Ac resisting high excess of sodium periodate.[43]

The amount of sialic acid oxidized, 0.2 and 0.33 µmol mg^{-1} by 1 and 2 mм sodium periodate, were in good agreement with the 0.16 and 0.31 µmol mg^{-1} of aldehyde produced in the reaction. This indicates that sodium periodate specifically targets sialic acid at low concentration. With increasing concentrations of sodium periodate, the sialic acid content was unchanged, while the amount of aldehyde created increased, suggesting sodium periodate targets almost exclusively other sugars at higher concentrations, such as hexosamines, galactose, and mannose indicated in a former study.[44] With a 1 mм concentration of sodium periodate, we retain 70% of Neu5Ac on mucins while generating a sufficient number of aldehyde groups. This condition was thus employed to oxidize BSM glycans, and the un-reacted aldehydes remaining after conjugating Tz or Nb were consumed by adding TRIS to avoid possible toxicity.

After reaction of the aldehyde with amine groups of Tz and Nb derivatives, the dialyzed product was analyzed by NMR. As shown in Figure 2D, the peaks at 7.15 to 7.7 ppm for Tz and peaks at 5.8 to 6.2 ppm for Nb confirmed their successful conjugation onto mucins. We then adjusted the amount of the Tz and Nb grafted on Glyn-Glyn to match those obtained with Prot-Prot through a series of iterations consisting in adjusting the concentration of Tz and Nb added into the oxidized BSM and monitoring the resulting amount of Tz and Nb on BSM by qNMR (**Table 1**). The similar amounts of Nb and Tz grafted onto

Table 1. The quantity of tetrazine and norbornene on BSM.

| Sample	Prot-BSM-Tz	Glyn-BSM-OTz	Prot-BSM-Nb	Glyn-BSM-Nb
Tz or Nb on BSM (μmol mg^{-1})	0.15 ± 0.03	0.16 ± 0.02	0.22 ± 0.02	0.21 ± 0.04

Prot-Prot and Glyn-Glyn ensures that the average crosslinking density does not impact the material and biological properties of the resulting gels and helps isolate the effect of crosslinking localization. Neither the formation of activated carboxylic groups by EDC nor the presence of aldehyde groups led to significant inter-mucin crosslinking. Indeed, BSM-Prot-Nb, BSM-Glyn-Tz, and unmodified BSM have a similar weight average molecular weight (M_w) around 1.1 MDa and a polydispersity (P_d) of around 1.9 (Figure S3, Supporting Information). Both the iminium ions resulting from the conjugation of Nb and Tz to aldehydes and the capping of unreacted aldehydes with TRIS could affect the polarity of the mucins. This could in turn affect the interactions of molecules and cells with the mucin materials. However, the zeta potential of all components were similar with values in the range of −20 mV (Figure S4, Supporting Information), suggesting no significant impact of such ions on the overall mucin charge.

2.2. Crosslinking Localization Affects Gelation Kinetics

We then investigated the mechanical properties of hydrogels, which are crucial characteristics that impact several aspects of biomaterials performance, including their interactions with cells.[45] The Prot-Prot gel (**Figure 3**A) switched from a loss modulus-dominated (G'') to storage modulus-dominated (G') response after 2 min, indicating the formation of viscoelastic gels. Both G' and G'' increased rapidly over 20 min and reached a plateau after 60 min, which suggests that most of the crosslinking reactions had occurred. A frequency sweep was performed with the same gels having reached the plateau to check the frequency-dependent viscoelasticity. G' dominated in the 0.01 to 10 Hz frequency range and the G' increased 2.5 times from 0.01 to 10 Hz. In the case of Glyn-Glyn gels (Figure 3B), the storage modulus was dominant over the loss modulus from the beginning of the measurement, indicating that a gel had already started to form after mixing. G' and G'' increased more slowly than for Prot-Prot gels, reaching a plateau value around 120 min after the start of the measurement.

As shown in Figure 3C, self-standing mucin hydrogel can be formed via both crosslinking. Given that similar Tz and Nb amounts are grafted on the mucins, and that the crosslinking reaction led to the same amount of surplus Nb (Figure 3D), we conclude that the degree of crosslinking was similar in both gels. The differences in gelling kinetics could be explained by differences in the accessibility of the Tz and Nb. Indeed, mucin protein backbones might be maintained in close proximity through hydrophobic interactions which would confine the Tz and Nb and facilitate the click reaction. The glycan chains are relatively flexible chains located along the long protein backbone, which could limit the probability of Tz and Nb encountering each other, thus limiting the gel formation speed. The smaller gap between storage modulus and loss modulus for
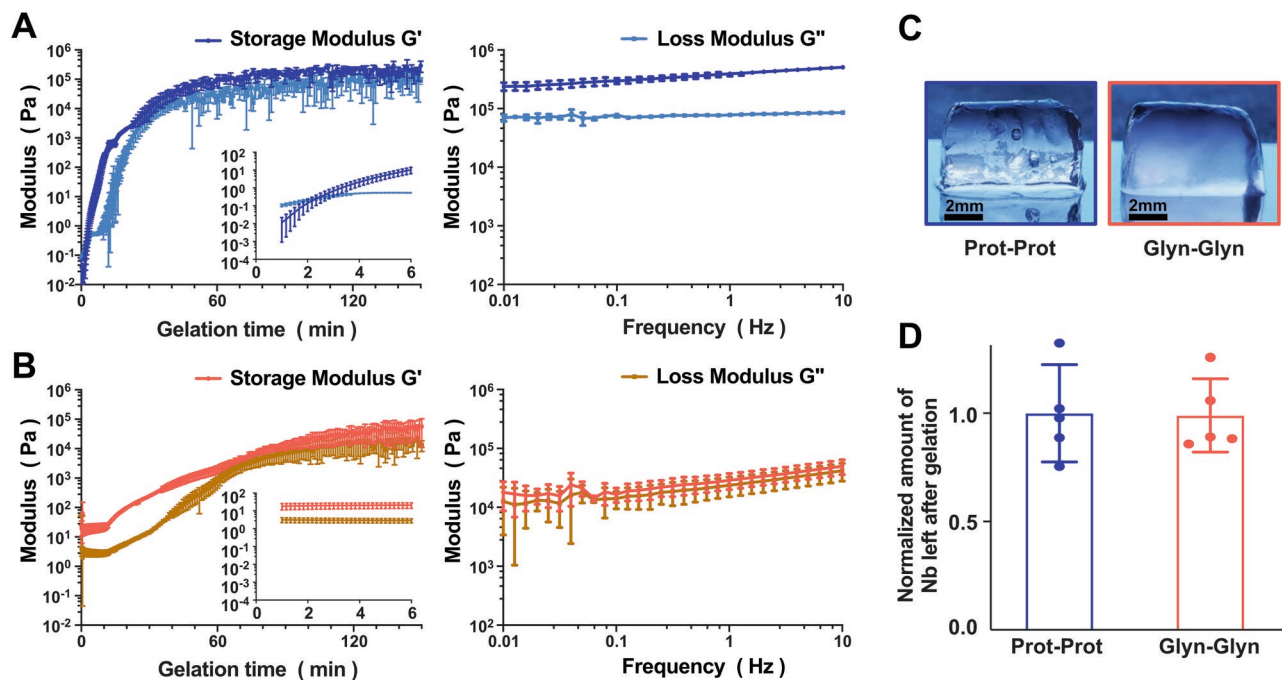
Figure 3. Rheological characterization of Protein-Protein and Glycan-Glycan mucin gels. Time-dependent rheological measurements of the mixed A) Prot-BSM-Tz and Prot-BSM-Nb (left) or B) Glyn-BSM-Tz and Glyn-BSM-Nb (left) in PBS. Final frequency-dependent viscoelastic moduli of the cross-linked Prot-Prot gel (right) and B) Glyn-Glyn gel (right). C) The gel images of Prot-Prot gel (left) and Glyn-Glyn gel (right). D) The relative amount of remaining norbornene groups in the two gels. The error bars indicate the standard deviations as obtained from measurements of n = 3 independent samples.

Glyn-Glyn gels compared to Prot-Prot gels could originate from crosslinked glycan chains in Glyn-Glyn gel being softer than the crosslinked protein backbone in Prot-Prot gel.[46] The mean plateau values of G' for Prot-Prot gel and Glyn-Glyn gel are 205 and 57 kPa respectively. However, the 3.5 fold difference in average storage and loss moduli are within the error margin of rheology measurements for soft heterogeneous materials such as these hydrogels.

2.3. Crosslinking Localization does not Affect Gel Permeability to Dextran

Crosslinking of polymeric networks can change the local architecture of a hydrogel, which in turn affects its interactions with other molecules. Here, we tested the diffusion of FITC labeled dextrans (F-dextran) with different molar masses and different hydrodynamic diameters (D_H)[47] into the gels (**Figure 4**) and calculated their diffusion coefficients, shown in **Table 2**. Dextran diffused in similar ways into both gels, with a maximum diffusion distance after 1 h of 2500 µm for 4 kDa dextran and 2000 µm for 10 kDa dextran. The 4 and 10 kDa dextrans continuously diffused forward into the mucin gel over the 60 min. For the 70 kDa dextran, the fluorescent intensity dropped rapidly within 50 µm and the diffusion front moved slowly after 30 min. The calculated diffusion coefficients for dextrans (Table 2) were nearly the same for the two gels. This similar diffusion coefficient suggests that the two gels have

some similarities in the architecture of the mucin, which is also supported by the similar crosslinking degree for the two gels. It was previously reported that the gel permeability and microstructure are related to their rheological properties,[48,49] which is in agreement with the similar permeability to dextrans and rheological properties measured for the two gels.

2.4. Crosslinking Localization Affects Gel Susceptibility to Proteases

As suggested by the differences in gelling kinetics, crosslinking localization seems to affect the accessibility of mucin domains. Thus, it is reasonable to assume that the crosslinking of mucin molecules could affect its accessibility to enzymes. Here, we tested the degradation process of the gels against two enzymes, trypsin which targets the protein backbone, and a mixture of O-glycosidase and neuraminidase which cleave O-linked sugars from mucins. The gels were labeled with a tetrazine-functionalized fluorescent dye and they are stable in PBS at 37 °C for at least 24 h (Figure S5, Supporting Information). The labeled gels are then exposed to trypsin or mixture of O-glycosidase and neuraminidase. The remaining fluorescent intensity of the gels was plotted over time (**Figure 5**A,D). When exposed to trypsin, the Prot-Prot gels took 10 h to degrade fully. The gels first degraded slowly with a 20% decrease of fluorescence intensity over the first 3.5 h, then followed a sharp acceleration of the degradation. In contrast, Glyn-Glyn gels degraded fully within 90 min.
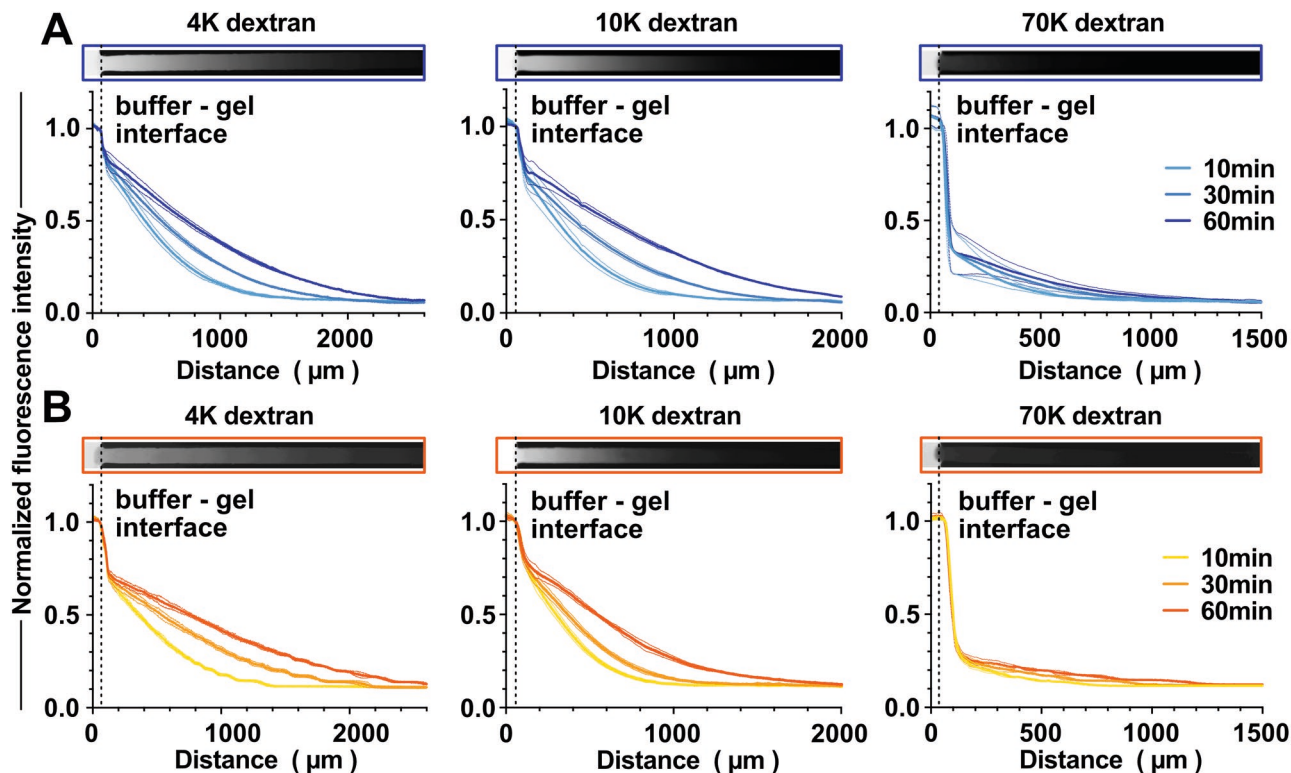
Figure 4. Diffusion of FITC labeled dextrans of 4, 10, and 70 kDa to A) Prot-Prot gel and B) Glyn-Glyn gel. The graphs are normalized fluorescence intensity along the mucin hydrogel channel and the inserted images are cropped from the images of dextran diffused for 1 h. The error lines indicate the standard deviations as obtained from measurements of $n = 3$ independent samples.

**ADVANCED
SCIENCE NEWS**

www.advancedsciencenews.com

**ADVANCED
FUNCTIONAL
MATERIALS**

www.afm-journal.de

Table 2. Diffusion coefficient of dextrans to the two mucin gels (no statistical significance between the two gels for all the three dextrans by one-way ANOVA analysis).

| Dextrans	4K- $D_H =$ 2.8 nm/[μm^2 s^{-1}]	10K- $D_H =$ 4.6 nm/[μm^2 s^{-1}]	70K- $D_H =$ 12 nm/[μm^2 s^{-1}]
Prot-Prot	171.6 ± 16.9	104.4 ± 14.7	3.3 ± 1.3
Glyn-Glyn	175.3 ± 20.0	85.5 ± 5.4	4.8 ± 1.8

The products of fully degraded gels obtained 3 days after addition of trypsin were then analyzed with SDS-PAGE (Figure 5B). The mucin fractions of Prot-Prot gels remained larger than 250 kDa, while Glyn-Glyn gel degradation generated a spread of fragments from 250 to 10 kDa. Bands from Glyn-Glyn degradation between 70 and 10 kDa were not stained by Schiff Reagents suggesting they correspond to non-glycosylated protein fraction. O-glycosidase can cleave O-linked glycans of mucins if combined with a sialic-acid removing neuraminidase.[50] However, neither of the two gels degraded when exposed to the mixture of O-glycosidase and neuraminidase. Only a minor decrease in fluorescence intensity of 3% for Prot-Prot and 5% for Glyn-Glyn after 24 h (Figure 5D) was measured, which concurred with the small amounts of released sugars detected (Figure 5E). There were more sugars released by O-glycosidase from Glyn-Glyn than from Prot-Prot gels (Figure 5E) after 24 h.

The crosslinking of mucin by protein backbone could cause steric hindrance that prevented access of proteases to their substrates and thereby slow down the proteolytic degradation of the gel and keep the mucin fragments large. In contrast, Glyn-Glyn crosslinking would leave the substrate open for trypsin to access and cleave the non-glycosylated protein core (Figure 5C). We expected Glyn-Glyn crosslinked gels to degrade when exposed to O-glycosidase and neuraminidase. However, very little sugar seems to be cleaved off from both gels by the enzymes. This might be because of the low efficiency of O-glycosidase against mucin gels since O-glycosidase can only cleave short saccharides such as disaccharides Galβ1-3GalNA (core 1) and GlcNAcβ1-3GalNAc (core 3). In addition, we anticipate that given the large size of the O-glycosidase (147 kDa), it would not diffuse deep into the hydrogel, limiting it to act superficially.

2.5. Crosslinking Localization Affects the Gel Bioactivity toward Undifferentiated Macrophages

If the localization of crosslinks affects the accessibility of a protease, it is reasonable to assume that the presentation of ligands to cell surface receptors could also be affected. In particular, changes in the accessibility of sugar residues such as sialic acid could modulate the bioactivity of the mucin gels toward immune cells. The oxidized Glyn-Glyn gel components have 30% less Neu5Ac and 44% less Neu5Gc sialic acids than Prot-Prot gel components and unmodified mucins[17] (Figures S6 and S7A, Supporting Information). To isolate the possible effect of sialic acid presentation, rather than its concentration, we oxidized the Prot-Prot gel components
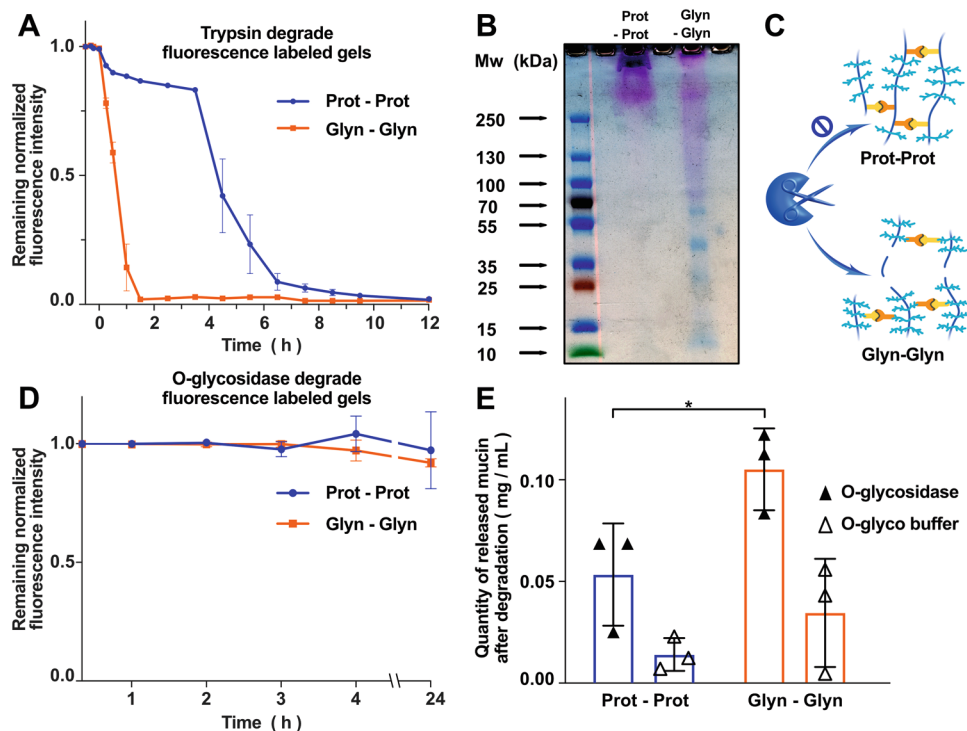
Figure 5. A) Degradation of the fluorescence labeled gels by trypsin; B) the SDS-PAGE analysis of fully degraded mucin gels by trypsin; C) Schematic graph for proteolytic degradation of protein-protein and glycan-glycan crosslinked mucin gels; D) degradation of the gels by O-glycosidase with neuraminidase; E) the released mucin concentration by O-glycosidase with neuraminidase and O-glyco buffer after 24 h. The error bars indicate the standard deviations as obtained from measurements of $n = 3$ independent samples. Statistical significance was calculated by one-way ANOVA test by Prism 8.0. * indicate p values of <0.05.
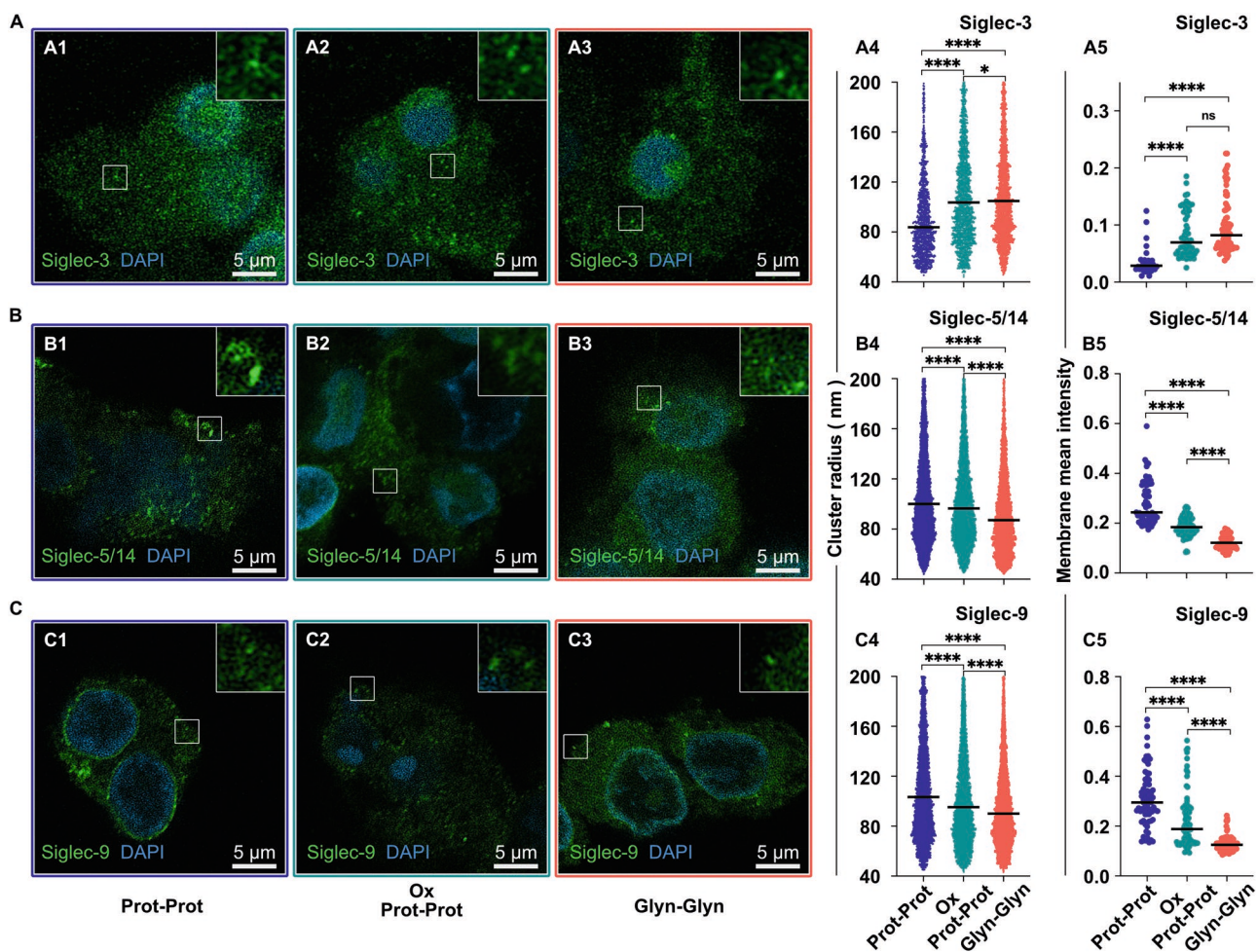
Figure 6. Immunofluorescence of Siglec surface receptors on THP-1-M0 after being cultured on Prot-Prot, Ox Prot-Prot and Glyn-Glyn for one day. Representative confocal images showing the Siglec-3 (in green) clustering on the membrane of macrophages on A1) Prot-Prot, A2) Ox Prot-Prot, and A3) Glyn-Glyn; B1) the Siglec-5/14 (in green) clustering on the membrane of macrophages on Prot-Prot, B2) Ox Prot-Prot and B3) Glyn-Glyn; C1) the Siglec-9 (in green) clustering on the membrane of macrophages on Prot-Prot, C2) Ox Prot-Prot, and C3) Glyn-Glyn; higher magnifications of selected clusters are shown in the upper right corner; all the cells were stained with DAPI (in blue). A4,B4,C4) The size of Siglec clusters with radius between 40 and 200 nm and A5,B5,C5) the fluorescence density on macrophages membrane were analyzed with the CellProfiler software. Measurements were performed on more than 80 cells and more than 1200 Siglec clusters in total were identified for each sample. Statistical significance was calculated by one-way ANOVA test by Prism 8.0 and *, **, ***, and **** indicate p values of <0.05, 0.01, 0.0005, and 0.0001, respectively.

(Ox Prot-Prot) to reach similar amounts of sialic acids as the Glyn-Glyn gel components (Figures S6 and S7A, Supporting Information).

To assess the bioactivity of the materials, THP-1 derived-M0 macrophages (THP-1-M0) were placed in contact with mucin hydrogels for one day. THP-1-M0 adhered to the TCP surface and formed small cell aggregates on all the three mucin gels (Figure S7B, Supporting Information). First, we investigated the expression level and localization of Siglec-3 (**Figure 6**A), Siglec-5/14 (Figure 6B) and Siglec-9 (Figure 6C) receptors at the membrane of the THP-1-M0 macrophages. The activation of sialic-acid binding Siglecs can result in a wide range of immune responses and are likely to further impact the expression levels of Siglecs themselves. The clustering of Siglecs at the membrane is an indirect evidence of substrate binding and it is thought to be important in regulating the downstream activity of Siglec binding.[41,51–54] This has been illustrated by

the artificial clustering of CD33 Siglec with antibodies, which induces the activation of immunoreceptor tyrosine-based inhibition motifs (ITIM) that affect cell activity including cytokine secretion.[55] The clustering of other inflammatory receptors including Dectin-1[56] and mannose receptors[57] strongly affect the intracellular signaling and inflammatory response.

Cells grown for one day on mucin gels were fixed and labeled directly on the gels to retain the morphology of the cell aggregate and preserve cell/material contact (Figure S8, Supporting Information). Confocal images (Figure 6-A1–A3, B1–B3, and C1–C3) showed that the cluster mean radius of Siglec-3 was larger on Glyn-Glyn than on Prot-Prot and Ox Prot-Prot gels (Figure 6-A4). In contrast, the cluster mean radii of Siglec-5/14 and Siglec-9 were smaller on Glyn-Glyn than on Prot-Prot and Ox Prot-Prot gels (Figure 6-B4,C4). Although cluster sizes detected ranged from 40 to more than 200 nm, the largest proportion of Siglec clusters were centered around 80 nm
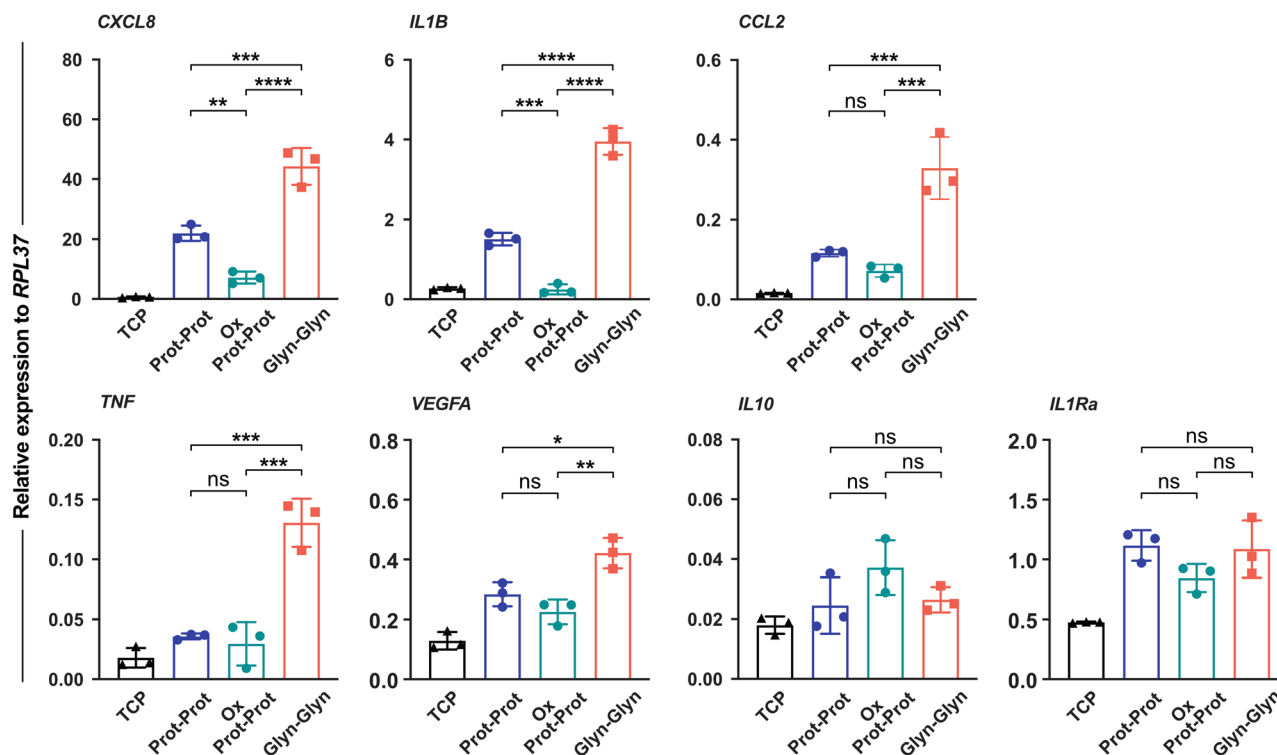
Figure 7. The gene expression of THP-1 derived macrophages after being cultured on TCP, Prot-Prot, Ox Prot-Prot, and Glyn-Glyn for one day. The data points indicate the mean of relative gene expression to *RPL-37* obtained from three independent experiments with duplicates. Statistical significance was calculated by one-way ANOVA test by Prism 8.0 and *, **, ***, and **** indicate *p* values of <0.05, 0.01, 0.0005, and 0.0001, respectively.

(Figure S9, Supporting Information). The expression levels of Siglec receptors on cell membranes as measured by the mean fluorescence density, showed a trend similar to Siglec clustering. Siglec-3 was more expressed on Glyn-Glyn and Ox Prot-Prot than on Prot-Prot gel (Figure 6-A5). In contrast, Siglec-5/14 and Siglec-9 were less expressed on Glyn-Glyn than on Prot-Prot and Ox Prot-Prot gels (Figure 6-B5,C5). These results suggest the crosslinking architecture of mucin gels has a profound effect on the expression and spatial regulation of key cell surface receptors known to module the activity of many immune cells. The Siglec expression and clustering on Ox Prot-Prot gels did not match those observed on Glyn-Glyn gels, highlighting the role of the crosslinking architecture. However, it was also not the same as on Prot-Prot gels suggesting a combined effect of oxidation and of the gel architecture.

The simultaneous interplay of Siglec expression, binding to substrate, clustering at the membrane, and intracellular signaling is complex. When integrated, these events lead to the upregulation or downregulation of inflammatory markers which we measured at the gene level by RT-PCR (**Figure 7**). The expression of pro-inflammatory cytokines for Glyn-Glyn, including CXCL8, IL1B, CCL2, TNF, and VEGFA was upregulated compared to both Prot-Prot and Ox Prot-Prot gels. The expression of anti-inflammatory cytokines, IL10 and IL1Ra, was similar among the macrophages on the three mucin gels. Overall, Glyn-Glyn gel induced a higher activation level of cytokines than its Prot-Prot counterparts. Here also, applying the oxidation step to Prot-Prot gel components did not lead to the increase in gene expression observed on Glyn-Glyn gels,

suggesting an important role of crosslinking architecture in the differences in M0 macrophage response.

We hypothesize that the localization of the crosslinkers on mucins directly affected the conformation of the mucin network in the gel which led to different Siglec clustering and expression level on the surface of macrophage membranes, and eventually to different activation profiles of the M0 macrophages. Crosslinking architecture can affect the arrangement of mucin molecules and thus the accessibility of sugar residues or glycans to receptors (**Figure 8**, top). Differences in mucin arrangements could also lead to different ligands densities, which in turn can affect Siglec clustering at the membrane (Figure 8, bottom). These results confirm that the details in how complex molecules such as mucins are presented to binders can strongly affect their interactions. This was also recently shown for surface-bound mucins and their binding to dextrans, antibodies,[58] and nanoparticles.[59]

3. Conclusions

The simple change of protein to protein versus glycan to glycan crosslinking of mucins strongly affected the susceptibility of the resulting gels to proteolytic cleavage and their immune-modulatory activities. For mucin biomaterial development, this discovery increases the portfolio of mucin materials variants at our disposal to modulate the immune system in defined ways, adding to the choice of mucin type and to glycomodulation by enzymatic treatment. Although the particular chemical diversity
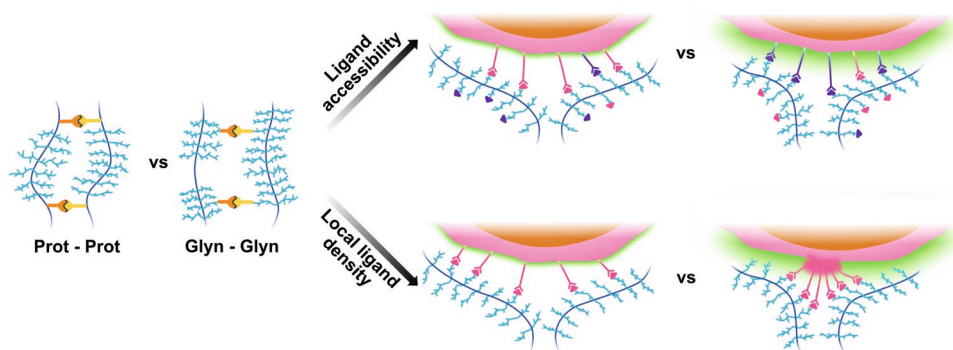
Figure 8. Illustration of mucin glycan interacting with cell surface receptors. The effects of crosslinking architecture on the accessibility of sugar residues or glycans to cell receptors (top), and the local ligands densities affecting cell receptors clustering (bottom).

and structure of mucins were uniquely suited to create these two distinct crosslinking architectures, the same approach could be attempted with other macromolecular assemblies, including hydrogels of proteoglycan, and structural proteins such as collagen and fibrin. In these systems, modulating the accessibility of key bioactive moieties could provide an additional degree of freedom in controlling their bioactivities, albeit in ways that are still unpredictable today.

4. Experimental Section

Materials: Tetrazine amine (Tz) and tetrazine oxyamine (OTz) were ordered from Bioconjugate Technology. 5-Norbornene-2-methylamine (Nb) was purchased from TCI EUROPE N.V. 6-Methyl-Tetrazine-BDP-FL were obtained from Jena Bioscience. Other chemicals came from Sigma Aldrich. PCR reagents and cell culture medium were obtained from Thermo Fisher Scientific. RNA purification kit was purchased from Qiagen and Human monocytes (THP-1) was ordered from ATCC. Trypsin crystalline was purchased from AMRESCO. O-Glycosidase (P0733S, $4 \times 10^{^7}$ U mL^{-1}) and α2-3,6,8 Neuraminidase (P0720S, $5 \times 10^{^4}$ U mL^{-1}) were ordered from New England Biolabs.

Functionalizing BSM with Tetrazine and Norbornene: The first method for conjugating Tz and Nb onto the mucin protein backbone was described in the former paper.[18] Briefly, bovine submaxillary mucin (BSM) was dissolved at 10 mg mL^{-1} in 0.1 M MES buffer with 0.3 M NaCl of pH 6.5. 1-ethyl-3-(3- dimethylaminopropyl) carbodiimide (EDC; 4 mmol per gram BSM) and N-hydroxysuccinimide (NHS; 4 mmol per gram BSM) were added into mucin solution and incubated at room temperature for 15 min. Then, tetrazine amine (Tz; 1 mmol per gram BSM) and 5-Norbornene-2-methylamine (Nb; 2 mmol per gram BSM) were added and the reactions were incubated at 4 °C overnight. The solutions were then transferred into a dialysis tube(Spectra-Por Float-A-Lyzer G2, MWCO 100 kDa) and dialyzed against 0.3 M NaCl for 2 days and then against MilliQ water for 1 day. Samples were lyophilized and stored at −20 °C. Materials for cell culture were filtered with a syringe filter (0.45 µm, Whatman GD/X 25) and transferred into tissue culture tubes (screw cap with 0.2 µm filter) before lyophilization, the samples were labeled as Prot-BSM-Tz and Prot-BSM-Nb.

Oxidation method for conjugating OTz and Nb onto mucin glycan chains: BSM was first dissolved at 5 mg mL^{-1} in oxidation buffer (OB; 0.1 M sodium acetate buffer, pH 5.5). Sodium periodate was then added into mucin solution to achieve a final concentration of 1×10^{-3} M or other indicated concentrations. The mixture was incubated on ice for 30 min protecting from light and then fivefold of ethylene glycol was added to quench the unreacted periodate at room temperature for 1 h. The mixture was then dialyzed (Spectra-Por Float-A-Lyzer G2, MWCO 100 kDa) against 0.3 M NaCl for two days and then against

sodium acetate buffer (50 × 10^{-3} M, pH 5) for one day. The oxidized BSM (OBSM) was transferred into tubes, and 5-Norbornene-2-methylamine (Nb; 2 mmol per gram BSM) with 50 × 10^{-3} M sodium cyanoborohydride, tetrazine oxyamine (OTz; 5 µmol per gram BSM) were added individually. The mixture was incubated at 4 °C for 48 h. Dialysis and lyophilization were performed the same way and the sample is labeled as Glyn-BSM-Nb and Glyn-BSM-OTz. The reduction of imine bond by sodium cyanoborohydride can generate stable nitrogen-carbon single bonds,[60] and the oximes formed between oxyamine of OTz and aldehyde are known to be more stable than imines.[61]

Quantification of Norbornene and Tetrazine Grafting by NMR: Samples (S, mg) were dissolved in 0.6 mL deuterium oxide with 30 × 10^{-3} M maleic acid. ^{1}H-NMR spectra were obtained with a Bruker Ultrashield plus 500 MHz spectrometer (Bruker Corporation, USA) and the data was processed with the MestReNova Software (version 12.0.4-22023). 6.285 ppm was selected as maleic acid peak, which is the shift of the two protons attached to the alkene and the integration area is labeled as M. Peaks within 7.15 to 7.7 ppm belong to the two protons on benzene far away from the tetrazine ring and 5.8 to 6.2 ppm belong to the 2 protons attaching to sp2 alkene in norbornene. The integration areas within 7.15 to 7.7 ppm and 5.8 to 6.2 ppm were labeled as T and N. The quantity of tetrazine (µmol mg^{-1}) on BSM (Qt) and norbornene (µmol mg^{-1}) on BSM (Qn) are calculated by equations: $Qt = \frac{T \times 18}{M \times S}$ and $Qn = \frac{N \times 18}{M \times S}$; the 18 indicate the 18 µmol maleic acid in the solution.

Sialic Acid Quantification: The Neu5Ac and Neu5Gc contents in BSM, oxidized BSM and functionalized derivatives were checked by high-performance anion-exchange chromatography (HPAEC). The samples were dissolved in MQ and then sialic acid was released by adding sulfuric acid (0.1 M) and reacting at 80 °C for 1 h.[62] Same amount of sodium hydroxide (0.1 M) was added to neutralize the solution and the samples were injected into the CarboPac PA1 column after filtration. Both Neu5Ac and Neu5Gc were eluted by a solution containing 33% of 0.3 M NaOH and 15% of 1 M sodium acetate, and the sugars were detected by pulsed amperometric detection (HPAEC-PAD) with an ICS-3000 system.[63,64]

Rheological Measurements: The rheological experiments were conducted on a commercial shear rheometer (MCR102, Anton Paar, Graz, Austria) equipped with a plate–plate measuring geometry. The gap between the measuring head (PP25, Anton Paar) and the bottom plate (P-PTD200/Air, Anton Paar) was set to 150 µm for all trials. The gel-components were diluted separately in PBS (pH 7.3) to a concentration of 25 mg mL^{-1}. Right before the measurements, the two gel components were mixed with equal mass proportions, vortexed for 30 s and 100 µL of the sample were pipetted onto the bottom plate. In a first measurement, gel formation was observed for a total time span of 150 min. Both the storage (G′) and loss (G″) moduli were measured in a torque controlled (M = 5 µN m) oscillatory (f = 1 Hz) trial. Afterward, a strain-controlled frequency sweep (fstart = 10 Hz, fend = 0.01 Hz) was conducted to assess the frequency dependent viscoelasticity of the crosslinked

sample. Therefore, a constant strain was used, which was chosen as the average of the five last strain values measured in the prior torque-controlled measurement. During all measurements, a liquid trap was used to prevent the sample from drying.

Diffusion Tests and the Calculation of Diffusion Coefficients: The diffusion tests were done within a microfluidic chip designed by Marczynski et al,[65] which is made of PDMS, consisting of finger-like channels and a reservoir channel. The gel components were dissolved separately in PBS (pH 7.4) at 25 mg mL^{-1} each and incubated at 4 °C overnight. The gel components were mixed at equal volume and the mixture was injected into the finger channels of the microchip immediately and stopped at the cross points. FITC labeled dextran solutions in PBS (0.1 mg mL^{-1}) were injected to the reservoir channel after the Prot-Prot gelation for 1 h and the GlynGlyn gelation for 2 h. Fluorescent images at several time points were taken with 4X objective using an inverted Nikon Eclipse Ti fluorescence microscope equipped with LED lamp (CoolLED pE-300). The exposure time of acquiring images was set to get no saturation pixels in the image. The images were then analyzed with ImageJ (open domain, version 1.52e). A rectangle area with a height of 40 pixels and length of 1500 pixels (1 pixel equal 2 µm) was chosen as the region of interest for each single "finger" of the "hand". This rectangle was placed at 40 pixels ahead of the mucin gel interface for each "finger", which is the area of dextran solutions serving as reference to normalize the fluorescent intensity. The diffusion coefficients[66] (*D*) were calculated based on the 50% fluorescent intensity points at 30 and 60 min by equation: $D = \left(\frac{X}{2 \times 0.476936}\right)^2 / T$ and *X* is the diffusion distance (µm), *T* is the time point (s).

Degradation Test: The gel-components were dissolved separately in PBS (pH 7.4) at 25 mg mL^{-1} each. The two gel components were mixed adequately by vortexing and pipetting up and down, and 50 µL samples were loaded into each well of a transparent 96 well plate (Greiner, f-bottom). After gelation at room temperature for 4 h, the gel was fluorescently labeled by adding 50 µL 6-Methyl-Tetrazine-BDP-FL (BODIPY FL; 10 µg mL^{-1} in PBS) and incubated at room temperature for 2 h protecting from light. The fluorescence intensity was read by a plate reader (Clario Star, BMG Labtech), with excitation wavelength of 479 nm with 14 nm bandwidth and emission wavelength of 524.5 nm with 27 nm bandwidth. To remove the free dye before treating with enzymes, labeled gels are washed by PBS until the fluorescent intensity does not decrease. For the degradation by trypsin, 50 µL trypsin of 10 µg mL^{-1} in PBS was applied into each well. For the degradation by glycosidase, gles was washed with MQ five times and then 5 µL O-glycosidase, 5 µL neuraminidase, 8 µL 10X glycobuffer and 32 µL MQ were added into each well. The degradation reaction was incubated at 37 °C, and gels were washed with PBS or glycobuffer 5 times and 100 µL PBS or glycobuffer was added into each well before reading fluorescent intensity at set time points. After reading, the same conditions of trypsin and glycosidase were used for further degradation.

Sodium Dodecyl Sulfate Polyacrylamide Gel Electrophoresis (SDS-PAGE): The fully degraded fractions of the two gels were analyzed by sodium dodecyl sulfate polyacrylamide gel electrophoresis (SDS-PAGE). To degrade the gels completely, trypsin(10 µg mL^{-1}) was added to the two gels in a transparent 96 well plate (Greiner, f-bottom) and then incubated for 3 days at 37 °C. The gels became a solution and was mixed with 5X SDS-PAGE protein loading dye in a ratio of 4:1. After thermal protein denaturation (95 °C for 5 min), the mixture was centrifuged at 9000 g for 2 min. 13 µL supernatant of each mixture was loaded onto a precast polyacrylamide gel (4–15% Mini-protein TGX precast protein gels, 15-well, 15 µL from BIO-RAD). Additionally, 4 µL of a protein standard solution (PageRuler plus prestained protein ladder from thermo scientific) was loaded onto a separate lane. The gel was run in an SDS running buffer (25 × 10^{-3} M TRIS-HCl, 200 × 10^{-3} M glycine, 0.1% w/v SDS; adjusted to pH 8.0) at 150 V for 45 min.

After the run, the gel was rinsed with MQ water for 1 min and then stained with 50 mL PageBlue protein staining solution (Thermo Scientific) for 1 h with gentle shaking at room temperature. And then the gel was rinsed with distilled water and incubated in a destained buffer (50% methanol in water with 10% acetic acid) until the background was clear.

After Coomassie staining, the gel was subjected to periodic acid-Schiff (PAS) staining to detect the glycans on mucin. For this purpose, the gel was first put into a fixing solution (25% Metanol, 10% acetic acid in MQ) for 1 h and then washed with MQ for 20 min with gentle shaking. The gel was then oxidized in 2% periodic acid solution for 15 min at room temperature and washed with MQ water 2 min for 2 times. The oxidized gel was then stained with Schiff reagent for 40 min at room temperature protecting from light. The gel was then washed with MQ water until getting a clear background and image of the gel was taken by CanoScan 4200F.

Schiff Assay: The schiff assay was performed following a published protocol[67] in a 96 well plate (Greiner, f-bottom). 120 µL freshly prepared solution of 0.06% periodic acid in 7% acetic acid was added into a 25 µL mucin solution and mixed with pipette 5 times. The plate was sealed with a plastic film and incubated at 37 °C for 1.5 h. The plate was then cooled to room temperature and 100 µL of Schiff's reagent was added with mixing by pipette action. The plate was sealed again and shaken for 5 min and color was allowed to develop at room temperature for a further 40 min. The plastic seal was removed and absorbance read at 550 nm by a plate reader (Clario Star, BMG Labtech).

THP-1 Cell Culture and Differentiation: Macrophage type 0 (THP-1-M0) was produced by differentiating the human monocyte cell line THP-1 (ATCC). THP-1 was cultured in RPMI-1640 medium with 10% FBS and penicillin/streptomycin (100 U mL^{-1}) (complete medium) in a humidified incubator with 5% CO$_2$ at 37 °C. Then the cells were differentiated by culturing in the complete medium with phorbol 12-myristate 13-acetate (PMA, 150 × 10^{-9} M) for three days and then changed to complete cell medium without PMA for one day. The cells adhered on the tissue culture petri dish (TCP) after differentiation and the formation of macrophages were confirmed by checking macrophages markers in the former work.[17] The THP-1-M0 was detached from the plate by accutase and diluted into 10^5 cells mL^{-1} in complete medium after washing with complete medium. Gel components were dissolved in a complete cell medium at 25 mg mL^{-1} and incubated at 4 °C overnight. And then mucin gels can be formed in each well of the 96 well plate (TC plate, SARSTEDT) by mixing equal volumes of the gel components, and incubate at room temperature for 2 h. 100 µL THP-1-M0 (10^5 cells mL^{-1}) was seeded on empty wells, Prot-Prot, Ox ProtProt, and GlyGly gel. The cells were cultured for 1 day and lysed for measuring the gene expression.

Immunofluorescence Staining: 150 µL THP-1-M0 (10^5 cells mL^{-1}) was seeded on Prot-Prot, Ox ProtProt, and GlyGly gel in cell culture slide (8 well, MatTek Life Science) and cultured in a humidified incubator with 5% CO$_2$ at 37 °C for one day. Cells were fixed on the mucin hydrogel in two steps. 150 µL 4% paraformaldehyde in a PBS buffer (pH 7.4) was first added into the cell medium of each well without mixing and incubated for 10 min at room temperature. Then the solution was aspirated carefully and 150 µL 4% paraformaldehyde was added into each well and incubated for another 10 min at room temperature. The cells were washed by PBS for two times and blocked with 2% BSA in PBS for 1 h at room temperature. The cells were then incubated with the following antibodies (50 µL at 15 µg mL^{-1}): Siglec-3 (Mouse, R&D, MAB11371), Siglec-5/14 (Goat, R&D, AF1072) and Siglec-9 (Goat, R&D, AF1139) at 4 °C overnight. After washing with PBS twice, NorthernLights 637 Fluorochrome-labeled Donkey Anti-Mouse IgG (R&D, NL008, 1:200 dilution) and NorthernLights 493 Fluorochrome-labeled Donkey Anti-Goat IgG (R&D, NL003, 1:200 dilution) were used as secondary antibody respectively at 37 °C for 1 h. Then the nucleus was stained by DAPI (0.5 µg mL^{-1}) for 5 min. The cell culture chamber was removed from the slide and 90% glycerol in 1X PBS was added on top of the cell and the slide was sealed with coverslips. The samples were observed under a super-resolution confocal microscope (Zeiss LSM 900-Airy2) with 63X oil objective. For imaging of the same Siglec stained cell, all the microscopy settings were the same for all the different gels. The Siglec clustering and the intensity of Siglec across the whole membrane were analyzed by CellProfiler (4.0.5) based on more than 80 cells for each sample and more than 1200 clusters were identified for each sample.

Real-Time PCR for Gene Expression: The RNA of collected cells was purified by Qiagen RNeasy mini kit and then cDNA was synthesized using Superscript III polymerase (Invitrogen). The gene expression of each cDNA was tested by real-time PCR (CFX96 Touch, Bio-Rad) with TaqMan Gene Expression Master Mix (Thermo Fisher Scientific) and TaqMan probes. The detection was performed at the following cycling conditions: 2 min at 50 °C, 10 min at 95 °C, 15 s at 95 °C, 1 min at 60 °C, and then go to step 3 for 50 cycles. RPL37 was applied as the housekeeping gene for THP-1-M0.

Supporting Information

Supporting Information is available from the Wiley Online Library or from the author.

Conflict of Interest

The authors declare no conflict of interest.

[1] G. Petrou, T. Crouzier, *Biomater. Sci.* **2018**, *6*, 2282.
[2] M. Shan, M. Gentile, J. R. Yeiser, A. C. Walland, V. U. Bornstein, K. Chen, B. He, L. Cassis, A. Bigas, M. Cols, L. Comerma, B. Huang, J. M. Blander, H. Xiong, L. Mayer, C. Berin, L. H. Augenlicht, A. Velcich, A. Cerutti, *Science* **2013**, *342*, 447.
[3] S. Senapati, S. Das, S. K. Batra, *Trends Biochem. Sci.* **2010**, *35*, 236.
[4] E. Guaní-Guerra, T. Santos-Mendoza, S. O. Lugo-Reyes, L. M. Terán, *Clin. Immunol.* **2010**, *135*, 1.
[5] E. R. Cobo, V. Kissoon-Singh, F. Moreau, K. Chadee, *Mucosal Immunol.* **2015**, *8*, 1360.
[6] A. Wiede, W. Jagla, T. Welte, T. Köhnlein, H. Busk, W. Hoffmann, *Am. J. Respir. Crit. Care Med.* **1999**, *159*, 1330.
[7] M. S. Murphy, *Nutrition* **1998**, *14*, 771.
[8] R. R. R. Janairo, Y. Zhu, T. Chen, S. Li, *Tissue Eng., Part A* **2014**, *20*, 285.
[9] T. Crouzier, H. Jang, J. Ahn, R. Stocker, K. Ribbeck, *Biomacromolecules* **2013**, *14*, 3010.
[10] L. Lindh, I. E. Svendsen, O. Svensson, M. Cárdenas, T. Arnebrant, *J. Colloid Interface Sci.* **2007**, *310*, 74.
[11] O. Svensson, L. Lindh, M. Cárdenas, T. Arnebrant, *J. Colloid Interface Sci.* **2006**, *299*, 608.
[12] V. J. Schömig, B. T. Käsdorf, C. Scholz, K. Bidmon, O. Lieleg, S. Berensmeier, *RSC Adv.* **2016**, *6*, 44932.
[13] D. J. Thornton, J. K. Sheehan, *Proc. Am. Thorac. Soc.* **2004**, *1*, 54.
[14] C. V. Duffy, L. David, T. Crouzier, *Acta Biomater.* **2015**, *20*, 51.
[15] C. Nowald, A. Penk, H.-Y. Chiu, T. Bein, D. Huster, O. Lieleg, *Macromol. Biosci.* **2016**, *16*, 567.
[16] K. Joyner, D. Song, R. F. Hawkins, R. D. Silcott, G. A. Duncan, *Soft Matter* **2019**, *15*, 9632.
[17] H. Yan, M. Hjorth, B. Winkeljann, I. Dobryden, O. Lieleg, T. Crouzier, *ACS Appl. Mater. Interfaces* **2020**, *12*, 19324.
[18] H. Yan, C. Seignez, M. Hjorth, B. Winkeljann, M. Blakeley, O. Lieleg, M. Phillipson, T. Crouzier, *Adv. Funct. Mater.* **2019**, *29*, 1902581.
[19] A. Varki, P. Gagneux, *Ann. N. Y. Acad. Sci.* **2012**, *1253*, 16.
[20] O. Lieleg, C. Lieleg, J. Bloom, C. B. Buck, K. Ribbeck, *Biomacromolecules* **2012**, *13*, 1724.
[21] E. C. M. Brinkman-Van der Linden, A. Varki, *J. Biol. Chem.* **2000**, *275*, 8625.
[22] M. Ohta, A. Ishida, M. Toda, K. Akita, M. Inoue, K. Yamashita, M. Watanabe, T. Murata, T. Usui, H. Nakada, *Biochem. Biophys. Res. Commun.* **2010**, *402*, 663.
[23] M. Inoue, H. Fujii, H. Kaseyama, I. Yamashina, H. Nakada, *Biochem. Biophys. Res. Commun.* **1999**, *264*, 276.
[24] P. R. Crocker, J. C. Paulson, A. Varki, *Nat. Rev. Immunol.* **2007**, *7*, 255.
[25] P. R. Kuhl, L. G. Griffith-Cima, *Nat. Med.* **1996**, *2*, 1022.
[26] L. Fourel, A. Valat, E. Faurobert, R. Guillot, I. Bourrin-Reynard, K. Ren, L. Lafanechère, E. Planus, C. Picart, C. Albiges-Rizo, *J. Cell Biol.* **2016**, *212*, 693.
[27] H. J. Yan, T. Casalini, G. Hulsart-Billström, S. Wang, O. P. Oommen, M. Salvalaglio, S. Larsson, J. Hilborn, O. P. Varghese, *Biomaterials* **2018**, *161*, 190.
[28] B. Winkeljann, M. G. Bauer, M. Marczynski, T. Rauh, S. A. Sieber, O. Lieleg, *Adv. Mater. Interfaces* **2020**, *7*, 1902069.
[29] Z. J. S. Mays, T. C. Chappell, N. U. Nair, *ACS Synth. Biol.* **2020**, *9*, 356.
[30] D. C. Schoenmakers, A. E. Rowan, P. H. J. Kouwer, *Nat. Commun.* **2018**, *9*, 2172.
[31] L. M. Delgado, Y. Bayon, A. Pandit, D. I. Zeugolis, *Tissue Eng., Part B* **2015**, *21*, 298.
[32] N. Davidenko, S. Hamaia, D. V. Bax, J.-D. Malcor, C. F. Schuster, D. Gullberg, R. W. Farndale, S. M. Best, R. E. Cameron, *Acta Biomater.* **2018**, *65*, 88.
[33] R. M. Desai, S. T. Koshy, S. A. Hilderbrand, D. J. Mooney, N. S. Joshi, *Biomaterials* **2015**, *50*, 30.
[34] J. P. Draye, B. Delaey, A. Van de Voorde, A. Van Den Bulcke, B. Bogdanov, E. Schacht, *Biomaterials* **1998**, *19*, 99.
[35] X. Zhou, G. Yang, F. Guan, *Cells* **2020**, *9*, 273.
[36] A. P. Corfield, C. D. Corfield, R. W. Veh, S. A. Wagner, J. R. Clamp, R. Schauer, *Glycoconjugate J.* **1991**, *8*, 330.
[37] A. N. Samraj, O. M. T. Pearce, H. Läubli, A. N. Crittenden, A. K. Bergfeld, K. Banda, C. J. Gregg, A. E. Bingman, P. Secrest, S. L. Diaz, N. M. Varki, A. Varki, *Proc. Natl. Acad. Sci. USA* **2015**, *112*, 542.
[38] T. Angata, *Front. Immunol.* **2018**, *9*.
[39] V. Padler-Karavani, N. Hurtado-Ziola, Y. Chang, J. L. Sonnenburg, A. Ronagh, H. Yu, A. Verhagen, V. Nizet, X. Chen, N. Varki, A. Varki, T. Angata, *FASEB J.* **2014**, *28*, 1280.
[40] O. Blixt, B. E. Collins, I. M. van den Nieuwenhof, P. R. Crocker, J. C. Paulson, *J. Biol. Chem.* **2003**, *278*, 31007.
[41] M. S. Macauley, P. R. Crocker, J. C. Paulson, *Nat. Rev. Immunol.* **2014**, *14*, 653.
[42] G. Reuter, R. Schauer, C. Szeiki, J. P. Kamerling, J. F. G. Vliegenthart, *Glycoconjugate J.* **1989**, *6*, 35.
[43] R. Veh, A. P. Corfield, M. Sander, R. Schauer, *Biochim. Biophys. Acta* **1976**, *486*, 145.
[44] R. G. Spiro, *J. Biol. Chem.* **1964**, *239*, 567.

[45] A. K. Blakney, M. D. Swartzlander, S. J. Bryant, *J. Biomed. Mater. Res., Part A* **2012**, *100*, 1375.

[46] A. A. Mohamed, S. Hussain, M. S. Alamri, M. A. Ibraheem, A. A. Abdo Qasem, O. A. Alhaj, M. A. Alshuniaber, *J. Chem. Chem. Eng.* **2019**, *2019*, 4267829.

[47] FITC-dextran information, https://www.sigmaaldrich.com/content/dam/sigma-aldrich/docs/Sigma/Product_Information_Sheet/1/fd250spis.pdf.

[48] C. A. Grattoni, H. H. Al-Sharji, C. Yang, A. H. Muggeridge, R. W. Zimmerman, *J. Colloid Interface Sci.* **2001**, *240*, 601.

[49] J.-Y. Kim, J.-Y. Song, E.-J. Lee, S.-K. Park, *Colloid Polym. Sci.* **2003**, *281*, 614.

[50] E. Tokhtaeva, O. A. Mareninova, A. S. Gukovskaya, O. Vagin, *Methods Mol. Biol.* **2017**, *1594*, 35.

[51] S. V. Pageon, T. Tabarin, Y. Yamamoto, Y. Ma, P. R. Nicovich, J. S. Bridgeman, A. Cohnen, C. Benzing, Y. Gao, M. D. Crowther, K. Tungatt, G. Dolton, A. K. Sewell, D. A. Price, O. Acuto, R. G. Parton, J. Justin Gooding, J. Rossy, J. Rossjohn, K. Gaus, *Proc. Natl. Acad. Sci. USA* **2016**, *113*, E5454.

[52] H. Thiesler, J. Beimdiek, H. Hildebrandt, *Cell. Mol. Life Sci.* **2020**, https://doi.org/10.1007/s00018-020-03601-z.

[53] P. R. Crocker, T. Feizi, *Curr. Opin. Struct. Biol.* **1996**, *6*, 679.

[54] S. Spence, M. K. Greene, F. Fay, E. Hams, S. P. Saunders, U. Hamid, M. Fitzgerald, J. Beck, B. K. Bains, P. Smyth, E. Themistou, D. M. Small, D. Schmid, C. M. O'Kane, D. C. Fitzgerald, S. M. Abdelghany, J. A. Johnston, P. G. Fallon, J. F. Burrows, D. F. McAuley, A. Kissenpfennig, C. J. Scott, *Sci. Transl. Med.* **2015**, *7*, 303ra140.

[55] S. Estus, B. C. Shaw, N. Devanney, Y. Katsumata, E. E. Press, D. W. Fardo, *Acta Neuropathol.* **2019**, *138*, 187.

[56] H. S. Goodridge, C. N. Reyes, C. A. Becker, T. R. Katsumoto, J. Ma, A. J. Wolf, N. Bose, A. S. H. Chan, A. S. Magee, M. E. Danielson, A. Weiss, J. P. Vasilakos, D. M. Underhill, *Nature* **2011**, *472*, 471.

[57] J. Gan, Y. Dou, Y. Li, Z. Wang, L. Wang, S. Liu, Q. Li, H. Yu, C. Liu, C. Han, Z. Huang, J. Zhang, C. Wang, L. Dong, *Biomaterials* **2018**, *178*, 95.

[58] T. M. Lutz, M. Marczynski, M. J. Grill, W. A. Wall, O. Lieleg, *Langmuir* **2020**, *36*, 12973.

[59] F. Wan, M. Herzberg, Z. Huang, T. Hassenkam, H. M. Nielsen, *Acta Biomater.* **2020**, *104*, 115.

[60] R. F. Borch, M. D. Bernstein, H. D. Durst, *J. Am. Chem. Soc.* **1971**, *93*, 2897.

[61] J. Kalia, R. T. Raines, *Angew. Chem., Int. Ed. Engl.* **2008**, *47*, 7523.

[62] A. Varki, S. Diaz, *Anal. Biochem.* **1984**, *137*, 236.

[63] L. S. McKee, H. Sunner, G. E. Anasontzis, G. Toriz, P. Gatenholm, V. Bulone, F. Vilaplana, L. Olsson, *Biotechnol. Biofuels* **2016**, *9*, 2.

[64] A. Harazono, T. Kobayashi, N. Kawasaki, S. Itoh, M. Tada, N. Hashii, A. Ishii, T. Arato, S. Yanagihara, Y. Yagi, A. Koga, Y. Tsuda, M. Kimura, M. Sakita, S. Kitamura, H. Yamaguchi, H. Mimura, Y. Murata, Y. Hamazume, T. Sato, S. Natsuka, K. Kakehi, M. Kinoshita, S. Watanabe, T. Yamaguchi, *Biologicals* **2011**, *39*, 171.

[65] M. Marczynski, B. T. Käsdorf, B. Altaner, A. Wenzler, U. Gerland, O. Lieleg, *Biomater. Sci.* **2018**, *6*, 3373.

[66] B. T. Henry, J. Adler, S. Hibberd, M. S. Cheema, S. S. Davis, T. G. Rogers, *J. Pharm. Pharmacol.* **1992**, *44*, 543.

[67] M. Kilcoyne, J. Q. Gerlach, M. P. Farrell, V. P. Bhavanandan, L. Joshi, *Anal. Biochem.* **2011**, *416*, 18.